energy&fuels
Article
pubs.acs.org/EF

Characterization of Modified Biochars Derived from Bamboo Pyrolysis and Their Utilization for Target Component (Furfural) Adsorption

Yunchao Li, Jingai Shao, Xianhua Wang,* Yong Deng, Haiping Yang, and Hanping Chen

State Key Laboratory of Coal Combustion, Huazhong University of Science and Technology, Wuhan 430074, China

ABSTRACT: Biochar (BC) derived from bamboo pyrolysis and its modified forms were treated with chemical methods (oxidation either by $KMnO_4$ or HNO_3 and base treatment with NaOH) and heat method. BC and modified BCs were investigated as adsorbents for target component (furfural) removal from aqueous solution. The samples were characterized to assess the effects of different treatments on structure and surface chemistry of BCs. The results show that chemical treatments increase the hydrophilicity of BC, whereas heat treatment causes the opposite effect. Oxidation treatment leads to the introduction of a large number of acidic functional groups on the BC surface, with HNO_3 being more effective than $KMnO_4$. In contrast, NaOH treatment and heat treatment increase the basicity of BC. Pore structures of BCs are also significantly changed after these modifications. Furfural adsorption capacity of BCs increases with the increase of basic surface group content, which can be attributed to the enhancement of dispersion interactions. The higher hydrophilicity of BC is, the lower the furfural uptake capacity is. The heat-treated samples demonstrate the highest capacity for furfural adsorption, with a removal efficiency of up to 100% at a furfural concentration of 10 g/L. However, all chemical treatments reduce furfural removal capacity. The Ho's pseudo-second-order model, intraparticle diffusion model, and Langmuir isotherm fit the adsorption data well.

1. INTRODUCTION

Due to the limited reserve of crude oil and increasing emissions of greenhouse gas, renewable biofuels, such as bioethanol, have attracted significant research attention nowadays.[1] The lignocellulosic biomass is a promising alternative feedstock to produce bioethanol,[2] as it primarily consists of hemicellulose and cellulose that are polysaccharides (polymers of five or six carbon chain sugar).[3] These polysaccharides can be depolymerized into fermentable sugars through three main process technologies: enzymatic hydrolysis, acid hydrolysis, and pyrolysis process.[4] However, a major challenge faced in commercial production of lignocellulosic bioethanol is that the inhibitor compounds would inevitably be generated during the conversion of biomass,[5] which are toxic to fermentation species. Furfural is one of the typical fermentation inhibitors, restricting the growth of microorganisms that are essential for bioethanol production.[5]

Various studies on the removal of furfural from the hydrolyzates or pyrolysis oil had been conducted, and sorption was proven to be an efficacious method.[3] Researchers had used various adsorbents for furfural removal, including activated carbons,[6−9] polymeric resins,[10,11] nanoporous adsorbent,[12] and fly ash.[13] However, the utilization of sorption was usually limited by high cost or poor efficiency of adsorbents. Biochar is a carbon-rich byproduct from the thermochemical conversion of biomass in the absence of oxygen. Due to its porous structures and cost-effectiveness, biochar has been used for contaminant management in water and soil.[14] Mohan et al.[15] had reviewed the use of biochar as adsorbent for the removal of inorganic and organic contaminants from water solution. In our previous study,[16] we also used a low-cost biochar (Bamboo charcoal, BC) for furfural removal from the model compounds of bio-oil. It was found that BC could selectively adsorb furfural despite the presence of sugars. The furfural removal efficiency by BC at equilibrium could be up to 60% in a furfural concentration of 10 g/L at room temperature, much higher than the removal efficiency of glucose that is only less than 5%. However, the furfural concentration after treatment in the model compounds of bio-oil was still very high.

Since raw BC adsorbents are not quite effective, these carbon materials need further modification for targeted adsorption. Yin et al.[17] comprehensively reviewed the modifications of activated carbon (including chemical, physical, and biological techniques) to enhance contaminant uptakes from aqueous solutions. Both the beneficial and the negative effects of modification techniques on the adsorption of targeted contaminant were found to be significant. Wibowo et al.[18] investigated the adsorption of toluene and benzene by activated carbon and the modified forms (chemical treatment using nitric acid and heat treatment under N_2 flow) and found that treatment with HNO_3 reduces adsorption capacity due to the introduction of a notable number of oxygenated acidic functional groups on the carbon surface. In contrast, thermal treatment greatly increased adsorption capacity due to the increase in basicity of the activated carbon. Several studies had been performed on BC modification. Wang and Yan[19] investigated the modification of BC using H_3PO_4, HNO_3, KOH, and $ZnCl_2$ and found that activating BC by H_3PO_4 was the best modification method for dye (DY-161) removal. Fan et al.[20] carried out experiments on the adsorption of chloramphenicol (CAP) from wastewater using BC and chemically modified BC (treated with H_2SO_4 and NaOH solutions). They observed that CAP adsorptions onto

Received: April 1, 2014
Revised: July 15, 2014
Published: July 15, 2014

dx.doi.org/10.1021/ef500725c | *Energy Fuels* 2014, 28, 5119−5127

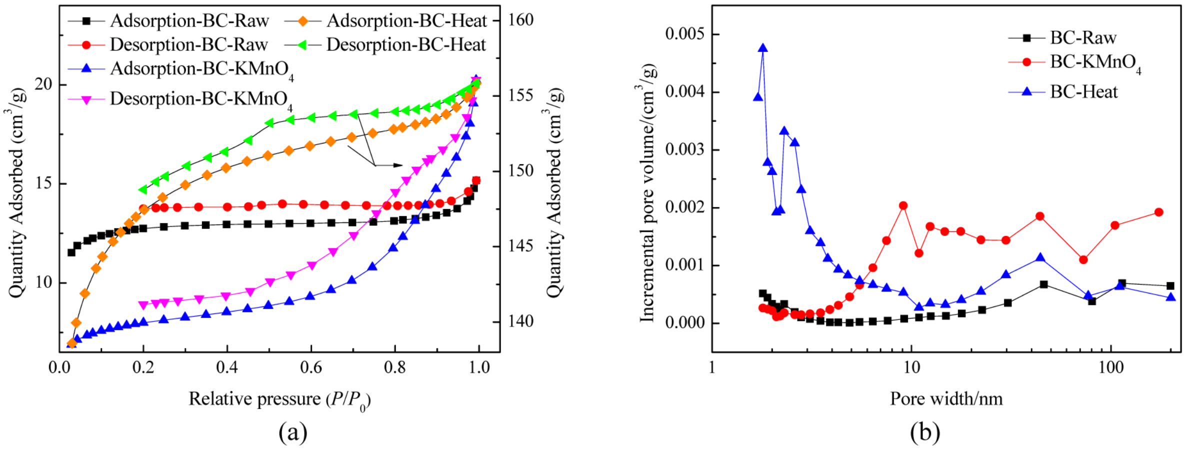

Figure 1. Pore structure characterization of BCs. (a) N_2 adsorption and desorption isotherms at 77 K for BCs, (b) pore size distributions calculated by the BJH method based on the N_2 adsorption data at 77 K for BCs.

the original BC and the H_2SO_4-treated samples were very minimal, whereas that onto the NaOH-treated BC was markedly more effective. Wang et al.[21] found that the adsorption capacity of Pb(II) significantly increased from 25.03 mg/g to 55.56 mg/g after $KMnO_4$ treatment of BC under microwave irradiation. Various chemical reagents had been used to modify BC surface for contaminant removal. Nevertheless, a systematic detailed characterization on different acid/base modifications and on heat-treated BCs has not yet been conducted. Furthermore, the effects of different treatments on the targeted adsorption for furfural removal by BCs need to be investigated.

In order to develop a low-cost and highly efficient adsorbent for furfural removal, in this study, BC was modified by chemical treatments and heat treatment to produce samples with different pore structures and surface characteristics. The premise is that the pore structures and the surface chemical characteristics are the key factors in controlling the sorption process. The adsorptive removal of furfural using BC samples with and/or without treatments was investigated and compared. A series of characterizations for BCs were performed, including CHN elemental analysis, N_2 adsorption−desorption, Fourier-transform infrared spectroscopy (FIIR), and Boehm titration. The effects of the physical and chemical properties of the adsorbents on the furfural removal mechanism are discussed. In addition, the kinetics of the adsorption is studied. Following our previous work that studied the use of biochar for fermentation inhibitor removal, this work focuses on the various treatments of biochar that may enhance the adsorption efficiency of furfural.

2. MATERIALS AND METHODS

2.1. Materials. Raw BC was obtained from pyrolysis of bamboo pieces in a fluidized bed reactor. The operating temperature was about 823 K, and the preparation method has been presented in detail in the literature.[22] The raw BC used here (BC-Raw) is the same as we used before.[16] Furfural was purchased from Jin Shan Ting Xin Chemical Ind., Ltd. (Shanghai, China). The compound was of analytical grade and its purity was greater than 99%.

2.2. Modified BC Preparation. In order to prepare modified BC, oxidation treatment using HNO_3 and $KMnO_4$, base treatment using NaOH, and heat treatment were performed on the BC-Raw samples.

2.2.1. Oxidation Treatment. The oxidation treatments of BC were performed using 2% $KMnO_4$ solution and 2 M HNO_3 solution at boiling temperature (about 373 K) for 24 h, respectively. The BC-to-solution ratio was 0.1 g/mL. The derived samples were washed with deionized water until they reached neutral pH. Then the samples were dried in an oven at 377 K for one night before usage. The oxidized samples are labeled as BC-$KMnO_4$ and BC-HNO_3, respectively.

2.2.2. Base Treatment. The base treatment of BC was carried out using 2 M NaOH for 24 h, following the same steps as the oxidation treatment discussed above. The base-treated sample is labeled as BC-NaOH.

2.2.3. Heat Treatment. Heat treatment for BC-Raw was performed in a horizontal tube reactor. About 20 g of BC-Raw was placed in the horizontal tubular reactor, and it was heated to the temperature of 1073 K under atmospheric nitrogen (300 mL/min flow rate). The heating rate was about 8 K/min. When the desired temperature (1073 K) was achieved, the samples were kept for 2 h. After the sample were cooled to room temperature, air was introduced into the horizontal tube reactor at a 300 mL/min flow rate and it was held for 1 h. By introducing air, new functional groups would be formed onto the BC surface. These groups were identified as basic pyrone-type groups resulting from the residual carbonyl group and the ether-type groups previously formed.[23] The heat-treated samples are hereafter referred to as BC-Heat.

2.3. Characterization of BCs. *2.3.1. Elemental Analysis.* A CHN elemental analyzer (EL-2, Germany) was used to determine the hydrogen, carbon, and nitrogen contents of the BCs. The oxygen content of the samples was determined by the difference.

2.3.2. Pore Structure Characterization. Nitrogen adsorption/desorption isotherms were measured at 77 K using an ASAP 2020 automatic instrument (Micromeritics, USA) to characterize the pore structure of the BCs. The surface area (S_{BET}) and the total pore volume (V_t) of the BCs were calculated using the Brunauer−Emmett−Teller (BET) method. Micropore surface area (S_{mic}) and micropore volume (V_{mic}) were determined using the *t*-Plot method. The pore size distributions of the BCs were determined by the Barrett−Joyner−Halenda (BJH) method from the adsorption isotherm data.

2.3.3. Fourier-Transform Infrared (FTIR) Spectroscopy Analysis. The Fourier transform infrared spectroscopy was obtained in the 4000−400 cm^{-1} frequency range using a VERTEX 70 spectrophotometer. The ratio of KBr powder to the sample was set to be 99:1, and the total weight of the mixture was 70 mg. The mixture was dried in an electrical oven at 378 K for 12 h before measurement.

2.3.4. Surface Acidic/Basic Determination. The amount of acidic/basic surface functions was determined using the Boehm method.[24] BC (0.5 g) was mixed with three different solutions: $NaHCO_3$, Na_2CO_3, and NaOH (50 mL; 0.05 M). The mixture was agitated at an orbital shaker for 24 h. Subsequently, 10 mL of the suspension was obtained and back-titrated with 0.05 M HCl. The surface acidity was calculated assuming that $NaHCO_3$ neutralized only carboxyl groups, Na_2CO_3 neutralized carboxyl and lactone groups, and NaOH neutralized all of the acidic groups including carboxyl, lactone, and

Table 1. Pore Structure Parameters of BCs

samples	$S_{BET}/(m^2/g)$	$V_t/(cm^3/g)$	$\bar{D}$/nm	$S_{mic}/(m^2/g)$	$V_{mic}/(cm^3/g)$	S_{mic}/S_{BET} (%)	V_{mic}/V_t (%)
BC-Raw	42.8	0.022	2.04	35.2	0.016	81.9%	74.4%
BC-$KMnO_4$	27.2	0.027	3.95	18.4	0.009	67.5%	31.5%
BC-HNO_3	0.5						
BC-NaOH	0.4						
BC-Heat	494.2	0.240	1.94	426.8	0.198	86.4%	82.8%

phenol groups.[18] Similarly, the amount of surface basicity of BCs was calculated by the consumption of HCl.

2.4. Adsorption Kinetic and Isotherm Experiment. The batch adsorption kinetic experiments were performed by adding a certain dose (m = 75 g/L) of BC into 100 mL of known furfural solution with initial concentration C_0 = 10 g/L contained in Erlenmeyer flasks (250 mL). The Erlenmeyer flasks were agitated in an orbital shaker at room temperature. At appropriate time intervals, the samples were collected and filtered, and the residual furfural concentration was analyzed at 277 nm using Lambda 35 UV-spectrophotometer (PerkinElmer, USA). The corresponding calibration curves were determined first. For adsorption isotherms, furfural solution of concentrations 5 g/L, 8 g/L, 10 g/L, 15 g/L, and 20 g/L were agitated with 75 g/L BC dose until equilibrium was reached. A control experiment was also performed without adding BC samples to check whether or not any adsorptive losses were caused by factors other than the adsorption process. All experiments were performed in duplicates.

3. RESULTS AND DISCUSSION

3.1. Characterization of Adsorbents. *3.1.1. Physical Property Analysis.* N_2 adsorption−desorption isotherms of BC-Raw, BC-$KMnO_4$, and BC-Heat at 77 K are plotted in Figure 1a. From the shape of the isotherm, it is clear that the treatment greatly affected the BC textural properties. The shapes of the isotherm for both BC-Raw and BC-Heat are close to type I according to the International Union of Pure and Applied Chemistry (IUPAC) classification, which is associated with microporous structures.[25] A hysteresis loop was observed at higher relative pressures near saturation, suggesting that both BC-Raw and BC-Heat mainly contained micropores, along with a certain amount of mesoporous and macroporous structures. Moreover, the saturated adsorption amount in BC-Heat increased, suggesting an increase in pore volume of the sample.[21] The shape of N_2 adsorption/desorption isotherms of BC-$KMnO_4$ can be classified as type II. The hysteresis loop is associated with mesopores of the char.[26] Compared with BC-Raw, a slightly higher adsorption amount of nitrogen was observed for the BC-$KMnO_4$ sample, probably due to the widening of micropores or with the opening of inaccessible pores during oxidation.[27]

Table 1 presents the surface area, the total pore volume, and micropore volume and average pore size of the BC samples, which suggested that the chemical treatments and heat treatment indeed caused significant changes on textural properties. The BC porosity data showed that the pores of BC-Raw were small, with the surface area of 42.8 m^2/g. After $KMnO_4$ treatment, surface area decreased but pore volume increased. The average pore width of BC-$KMnO_4$ also increased compared with that of BC-Raw. These results suggest that $KMnO_4$ oxidation could enlarge the micropores. The decrease in surface area may be due to the formation of oxidation products such as Mn oxides that block the pores of BC or cause the collapse of pore walls.[28] After HNO_3 treatment and NaOH treatment, respectively, the surface area and pore volume of both samples decreased significantly (surface area <1 m^2/g), making it impossible for the instrument to measure other pore parameters. As reported in previous studies, oxidation by HNO_3 could also cause the collapse of pore wall and the expansion of micropores into mesopores or macropores.[23,29] The generation of oxygen-containing functional groups after HNO_3 treatment on the micropores may also prevent the entering of nitrogen molecules.[30] Stavropoulos et al.[31] studied the influence of modification on activated carbons' porosity and surface structure and found that after HNO_3 treatment a significant decrease in surface area and pore volume was observed. They also found the longer the treatment time, the less the pore volume was. They attributed it to the introduction of oxygen functional groups in pore walls. It was also found that HNO_3 had erosive effects on carbon structure. Pradhan and Sandle[32] used different oxidants, i.e., H_2O_2, HNO_3, and $(NH_4)_2S_2O_8$, to modify activated carbons, and found samples treated with HNO_3 had the lowest surface area. The researchers proposed that the result could be caused by fixation of oxygen complexes. The decrease in surface area for BC-NaOH may be due to the blocking of Na^+ occlusion. Fan et al.[20] also modified bamboo charcoal with NaOH and found the modified BC had a surface area of less than 1 m^2/g with few micropores. The results shown in this study are consistent with the previous study.[20] Heat treatment at 1073 K resulted in maximum values of BC surface area and pore volume. Pore development took place simultaneously with the release of volatiles at high temperatures. The surface area and the total pore volume of BC-Heat were 494.2 m^2/g and 0.240 cm^3/g, respectively, which increased by over 1 order of magnitude relative to BC-Raw. Ahmad et al.[33] also confirmed that the surface area and the pore structure of BC were strongly affected by the treatment temperature. They found a significant increase in surface area for BC generated at 700 °C with a surface area of nearly 400 m^2/g, while for raw biomass the surface area was only 5.01 m^2/g. Most researchers have reported a maximum surface area was obtained at 650−850 °C for biochar.[34] It was found that higher temperature facilitated the formation of porous structures. Heat treatment enhanced the micropores because of the decomposition of the oxygenated functional groups that might either block the entrances of the micropores or reside in the micropores.[23]

To further illustrate the influence of chemical treatments and heat treatment on the structure of the samples, BC pore size distributions are presented in Figure 1b. It shows a wide pore size distribution and a slightly heterogeneous texture of BCs. Heat treatment apparently favors the formation of micropores, whereas $KMnO_4$ treatment may enlarge the micropores to mesopores.

3.1.2. Chemical Composition Analysis. 3.1.2.1. Elemental Analysis of BCs. Table 2 shows the elemental contents of the BCs. In general, in BCs treated with chemical reagents carbon content decreased but oxygen content increased relative to BC-Raw. In contrast, the effects of heat treatment were the opposite. The decrease in carbon content in BC-$KMnO_4$ and BC-HNO_3 may be caused by the formation of surface oxygen

Table 2. Elemental Compositions of BCs (wt %, Ash-Free Basis)

sample	C	H	N	O (by diff.)	H/C	O/C
BC-Raw	63.5	2.9	0.55	33.0	0.55	0.39
BC-$KMnO_4$	60.7	3.2	0.50	35.6	0.64	0.44
BC-HNO_3	56.7	3.1	2.6	37.7	0.65	0.50
BC-NaOH	59.5	3.0	0.24	37.2	0.60	0.47
BC- Heat	70.7	1.1	0.58	27.6	0.18	0.29

complexes from the oxidation of surface carbons.[32] Furthermore, the increase in nitrogen content of BC-HNO_3 may be caused by the formation of some nitro groups or by the irreversible adsorption of nitrate ions.[31,32] The changing trends in oxygen and carbon contents of BC after NaOH treatment are similar to those reported in the literature.[20] The increase in carbon content and the decrease in oxygen content for BC-Heat may result from further carbonization. Because H is primarily associated with organic matter, the molar H:C ratio can reflect the degree of carbonization or organic residues.[35] As shown in Table 2, chemical treatments increased the H:C ratio of BC, suggesting an increase in organic components, whereas heat treatment under N_2 atmosphere greatly reduced the amount of organic residues. The molar O:C ratio of the char should partially reflect the hydrophilicity of its surface.[36] The ascending order of O:C ratio for the BC samples is BC-Heat < BC-Raw < BC-$KMnO_4$ < BC-NaOH < BC-HNO_3, indicating a far more hydrophilic and higher polar group content of BCs. It should be noted that the high hydrophilicity of BC may lead to a competition for adsorption sites in BC between adsorbates (furfural) and water in solutions.

3.1.2.2. FTIR Analysis. The FTIR transmission spectra of BCs are shown in Figure 2. Table 3 lists the possible functional groups of BCs based on ref 37. The main bands of BC-Raw were identified at around 3426 cm^{-1}, 2921 cm^{-1}, 1580 cm^{-1}, 1430 cm^{-1}, 1375 cm^{-1}, 1240 cm^{-1}, 877 cm^{-1}, 812 cm^{-1}, 753 cm^{-1}, and 628 cm^{-1}, which is consistent with the previous study.[20] A strong peak was centered at 3426 cm^{-1}, which may be due to hydroxyl stretching region. A peak was also found at 2921 cm^{-1} because of the presence of aliphatic groups such as CH, CH_2, and CH_3.[33,38] The presence of significant bands in the respective spectra of BC-$KMnO_4$, BC-HNO_3, and BC-NaOH suggested that the main polar groups remained on the surface of BC after chemical treatments, although some differences were found among the bands of BCs. For BC-$KMnO_4$, a new peak was found at 581 cm^{-1}, which may be due to the stretching of Mn−O bond,[21] whereas the peak at 630 cm^{-1} disappeared. The FTIR spectra of BC-HNO_3 were somewhat different from those of BC-$KMnO_4$. New bands at 1704 and 1527 cm^{-1} were observed in the BC-HNO_3 spectrum, which may be due to the C═O stretching vibration from the carboxyl acid groups.[32] Nitro (-NO_2) stretching vibrations (1328 cm^{-1}) were found only after HNO_3 treatment. Adsorption intensities of C−O bonds (bands at 1260 cm^{-1}) increased in BC-HNO_3 compared with those in BC-Raw. For BC-NaOH, new peaks also emerged at 606 and 472 cm^{-1}, whereas bands at 1260 cm^{-1} disappeared, implying the presence of lactone and the absence of phenol because of the neutralization of hydroxyl by NaOH.[20,39] The FTIR spectrum of BC-Heat was quite different in shape and intensity from those of the other BC samples. The spectrum was very flat, which suggested that almost all the polar functional groups had decomposed after heat treatment. Ahmad et al.[33] also demonstrated that a higher pyrolysis temperature caused a further loss in the intensity of polar groups in biochar, leading to the condensation of aromatic units. The low contents of polar functional group led to a superhydrophobic characteristic of BC-Heat.

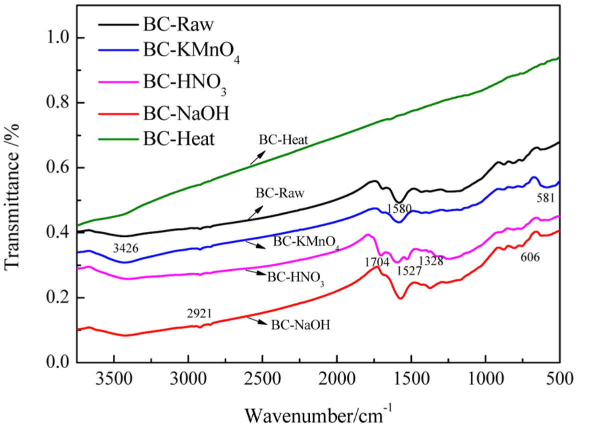

Figure 2. FTIR transmission spectra of the raw and modified BC samples.

3.1.2.3. Acid−Base Property Analysis. To obtain further information on the functional groups on BCs, acid−base titration was performed. Acidity/basicity manifested on the surface of BCs originated from the functional groups on the surface.[18] Some surface functional groups, such as carboxyl, lactone, and phenol groups, were sources of surface acidity,[40,41] whereas the carbonyl, chromene, and pyrone surface groups and the delocalized π electrons on Lewis basic sites on the basal planes of BC were sources of surface base.[23] Table 4 lists the quantitative analysis results of these functional groups for BCs. The amount of total acidity groups was 0.310 mmol/g for BC-Raw, composed of 0.125 mmol/g, 0.110 mmol/g, and 0.075 mmol/g of carboxyl, phenol, and lactone group, respectively. The amount of basic functional group was 0.175 mmol/g. Compared with BC-Raw, the number of acidic functional groups increased after oxidation treatment (BC-$KMnO_4$ and BC-HNO_3) but decreased after base treatment or heat treatment. For BC-$KMnO_4$, the total acidity of oxygen-containing functional groups increased by about 26%. The contents of phenol and lactone groups increased substantially after $KMnO_4$ treatment. The total basic functional groups in BC-$KMnO_4$ decreased by 25.7% compared with BC-Raw. The total acidity of BC-HNO_3 was the highest, whereas the basic functional group content was the lowest among all samples. This result demonstrated that HNO_3 was stronger than $KMnO_4$ in acidicity and oxidizing properties. As for base treatment, NaOH treatment increased the content of basic functional groups. The contents of carboxyl and phenol groups were significantly reduced after NaOH treatment because of the neutralization reaction. The lactone group content in BC-NaOH (0.155 mmol/g) was doubled compared with that of BC-Raw (0.075 mmol/g). The acid−base contents of BC and modified BCs were consistent with the FTIR results. Heat treatment reduced the acidic functional group content, suggesting that a deeper carbonization process occurred in BC-Heat. However, the basic functional group content increased in BC-Heat because of the formation of new basic functional groups,[18,24] as mentioned in section 2.2.3.

Table 3. Main Functional Groups of BCs

sample wave number (cm^{-1})[a]	BC-Raw	BC-KMnO$_4$	BC-HNO$_3$	BC-NaOH	functional groups	compounds
3200−3700	3426.34(s)	3432.74(s)	3409.37(s)	3429.16(s)	OH stretching	acid, methanol
2700−3000	2921.01(w)	2920.15(w)	2920.35(w)	2921.03(w)	C−H$_n$ stretching	alkyl, aliphatic
1700−1730			1703.79(m)		C=O stretching	carboxyl
1450−1600	1579.86(s)	1583.00(s)	1593.96(s), 1527.18(m)	1573.81(s)	C=O stretching	ketone and carbonyl
1420−1480	1429.17(w)	1432.45(w)	1426.99(w)	1427.88(w)	CH bending	aliphatic
1360−1430	1375.26(w)	1381.58(w)	1382.32(w)	1375.80(m)	OH, CH bending	Hydrocarbon, acid, phenol, olefin and alcohol
1320−1340			1328.16(w)		-NO$_2$	nitrogen
1200−1300	1239.09(w)	1262.63(w)	1251.78(m)		C−O stretching	aryl-alkyl ether linkage, phenol
700−900	877.10(m), 812.18(m), 753.17(w)	878.87(m), 813.06(m), 759.63(m)	812.98(m), 762.30(m)	875.68(m), 809.13(m), 756.92(w)	C−H	aromatic hydrogen
700−400	627.96(w)	581.07(s)	628.23(w), 587.72(w)	627.05(w), 606.41(w), 472.00(w)	C−C stretching or Mn−O	

[a] s: strong, m: medium, w: weak.

Table 4. Surface Organic Functional Groups of BCs

sample	basicity (mmol/g)	acidity (mmol/g)	carboxylic (mmol/g)	phenolic (mmol/g)	lactonic (mmol/g)
BC-Raw	0.175	0.310	0.125	0.110	0.075
BC-KMnO$_4$	0.130	0.390	0.125	0.145	0.120
BC-HNO$_3$	0.025	0.545	0.245	0.185	0.115
BC-NaOH	0.305	0.235	0.035	0.045	0.155
BC-Heat	0.275	0.190	0.050	0.055	0.085

In general, oxygen-containing functional groups, particularly the acidic groups of carbon, are hydrophilic. The high contents of acidic surface functional groups in BCs lead to high hydrophilicity of BCs, which tend to adsorb water. As shown in Table 4, the ascending order of acidic functional groups for the BC samples is BC-Heat < BC-NaOH < BC-Raw < BC-KMnO$_4$ < BC-HNO$_3$, which is similar to the results of hydrophilic analysis. In contrast, the amount of basic functional groups is positively correlated with the electronic density of basal planes.[31]

3.2. Adsorption Studies. Furfural was removed from aqueous solutions through targeted adsorption by BC-Raw and modified samples. As presented in Figure 3, the furfural adsorption capacity of BC-Raw was higher than that of chemically treated BC, but much lower than that of heat-treated BC. Furfural adsorption capacity onto biochar samples followed the ascending order: BC-HNO$_3$ < BC-KMnO$_4$ < BC-NaOH < BC-Raw < BC-Heat. The BC-Heat furfural removal efficiency can reach up to 100% at furfural concentration of 10 g/L. This result suggested that both oxidation and base treatments inhibited the removal of furfural, whereas heat treatment facilitated the removal of furfural. The possible reasons are discussed below.

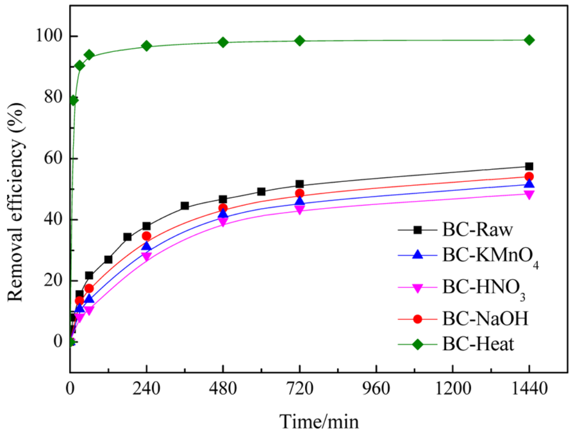

Figure 3. Adsorption of furfural onto BC-Raw and modified BCs. T = 298 K, m = 75 g/L, C_0 = 10 g/L.

As found in previous studies, the adsorption of organic compounds onto carbon materials depends on both physical and chemical properties of carbon.[42] Pore structures of BC influence the physical adsorption, among which surface area and pore volume are the most important factors. However, the surface chemistry of the carbon materials also plays important roles in affecting the adsorption of organic compounds, the charge of the surface, the electronic density and hydrophilicity of the chars.[18,43]

For physical adsorption, the surface area and micropore volume of BC-Raw were higher than those of chemically modified samples but significantly lower than that of heat-treated sample. The higher surface area and pore volume increased the adsorption capacity of furfural for BC-Heat; however, the decrease in surface area and pore volume was disadvantageous for furfural removal of chemically modified samples. In contrast, the adsorption capacities of BCs (BC-HNO$_3$ < BC-KMnO$_4$ < BC-NaOH < BC-Raw) were not exactly positively correlated with their surface areas or pore volumes (BC-NaOH < BC-HNO$_3$ < BC-KMnO$_4$ < BC-Raw, Table 1). Thus, the adsorption of furfural might be more significantly affected by the chemistry of the adsorbent surface in this study.

Two types of interaction occur between the adsorbent and the adsorbate during chemical adsorption: electrostatic interaction and dispersion.[23] Electrostatic interaction may occur when the adsorbate is dissociated. For dispersion, three mechanisms are proposed as follows: $\pi-\pi$ interaction, hydrogen bond, and electron donor–acceptor mechanism.[23] At the natural pH, furfural is in the molecular form; thus, only the dispersion interaction is expected to occur. The furfural has a structure similar to benzene ring, and the BC atoms are organized as an aromatic structure. Therefore, $\pi-\pi$ interaction may have a dominant effect on adsorption.[16,20] Taking the above analysis into consideration, the oxidation treatment (by $KMnO_4$ and HNO_3) is expected to reduce the furfural adsorption capacity because it increases the number of acidic groups but reduces the number of basic groups. The acidic functional groups in BCs could remove the π-electrons from the carbon matrix, leading to a reduction in the strength of the interaction between the furfural molecule and the carbon basal planes.[44] Comparing BC-HNO_3 with BC-$KMnO_4$, the former would have a lower adsorption capacity because BC-HNO_3 has a higher amount of acidic functional groups and fewer basic ones. Consequently, lower electronic density would lead to weaker dispersion interaction. Most published studies report a decreasing adsorption capacity of organic compound with increasing carbon surface acidic oxygen content,[23,45,46] and many researchers have also investigated the effect of Mn oxides on the adsorption of inorganic contaminant.[47,48] The Mn oxides on the surface of carbon may increase the hydrophilicity of samples; however, the interaction mechanism between Mn oxides and furfural molecules and its effects on the adsorption process remain unexplored. Apart from $\pi-\pi$ interaction, hydrogen bonding is another factor that influences chemical adsorption process. Competition occurs between water and furfural molecules for adsorption sites in BCs. The hydrogen bonds can form between water and the hydrophilic groups of BCs, which can produce clusters that will block the channel of furfural molecules into the micropores.[17] As mentioned in section 3.1.2.1, BC-HNO_3 is more hydrophilic than BC-$KMnO_4$; therefore, it may prefer adsorbing water to furfural molecules, resulting in lower furfural adsorption capacity. For the same reasons, a decrease in furfural uptake would also be expected for sample BC-NaOH relative to sample BC-Raw. However, for BC-NaOH, a furfural uptake larger than BC-HNO_3 and BC-$KMnO_4$ is observed because of an increase in the amount of π-electrons of the carbon matrix and a reduction in the amount of acidic functional groups. BC-Heat has the lowest concentration of surface acidic oxygen groups with least hydrophilicity, as well as the largest surface areas and highest micropore volumes. Thus, it has the highest adsorption capacity for furfural. Furthermore, Figure 3 shows that the adsorption capacities of BCs are positively correlated with their basicity in the same increasing order: BC-HNO_3 < BC-$KMnO_4$ < BC-Raw < BC-Heat. The result is consistent with the previous finding that dispersion interaction increases with the basicity of char.[18] As can be seen, the order was also consistent with the hydrophobic trend of the BCs. Despite the strongest basicity of the sample modified by NaOH, it only exhibits moderate furfural adsorption capacity (BC-$KMnO_4$ < BC-NaOH < BC-Raw < BC-Heat), which may be attributed to the conflicting effects of pore structure and surface chemistry. On the basis of the above analysis, the reasons for the adsorption trend of furfural by BCs can be schematized as shown in Figure 4.

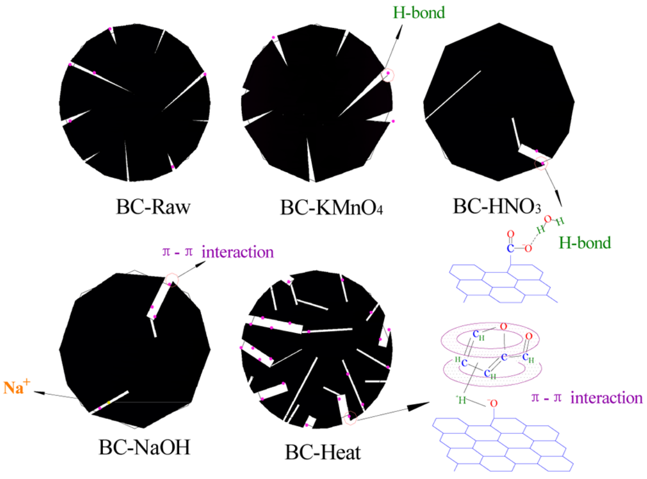

Figure 4. Effect of different treatments on adsorption of furfural by BCs.

3.3. Kinetics and Adsorption Isotherms Study.

Kinetic models were used to more comprehensively understand the adsorption process. The transient behavior of the system for furfural removal was analyzed using Lagergren's pseudo-first-order and Ho's pseudo-second-order models. The film diffusion model and intraparticle diffusion model were used to determine the rate-limiting step. The linear forms for Lagergren's model and Ho's model were $\lg(q_e - q_t) = \lg q_e - k_1 t/2.303$ and $t/q_t = 1/(k_2 q_e^2) + t/q_e$, respectively.[49] The film diffusion and intraparticle diffusion model were defined as $-\ln(1 - q_t/q_e) = k_b t$ and $q_t = k_{id} t^{1/2} + I$, respectively.

The adsorption isotherms were basically used to describe the interaction of adsorbent and solutes. Two extensively used isotherms (Freundlich and Langmuir isotherms) were selected. The Freundlich isotherm was usually adopted for nonideal adsorption systems, while the Langmuir isotherm was usually used for describing a monolayer adsorption that occurred on the surface of identical sites.[50] The linear forms for these two isotherms were $\lg q_e = \lg C_e/n + \lg K_F$ and $C_e/q_e = C_e/q_m + 1/(q_m K_L)$, respectively,[51,52] where C_e is the furfural concentration at equilibrium; n stands for the adsorption intensity and if $1/n < 1$, it means a favorable adsorption process. More details of these kinetic and isotherm parameters can be found in refs 16 and 52.

The applicability of the kinetic models and adsorption isotherms were evaluated using the linearized plots and the correlation coefficient (R^2) values. The diagrams for adsorption of furfural onto BCs are shown in Figure 5. Table 5 lists the corresponding parameters of the kinetic models and adsorption isotherms of different BCs. Figure 5a,b and Table 5 show that the Ho's pseudo-second-order model fits the experimental data better than the Lagergren's pseudo-first-order model during the entire adsorption time. The two-stage intraparticle diffusion model is more suitable for describing the adsorption process than the film diffusion model, suggesting that the rate-limiting step is the adsorbent phase diffusion (seen in Figure 5c,d). For adsorption isotherms, the Langmuir isotherm provides a better fitting than the Freundlich isotherm equation as seen in Figure 5e,f and Table 5. It suggests the adsorption feature of BCs is mainly a monolayer adsorption. The maximum adsorption capacity of furfural onto BC-Heat sample with the value of 253.16 mg/g is obtained from the calculation by the Langmuir isotherm. In addition, the values of $1/n$ for all of the BC

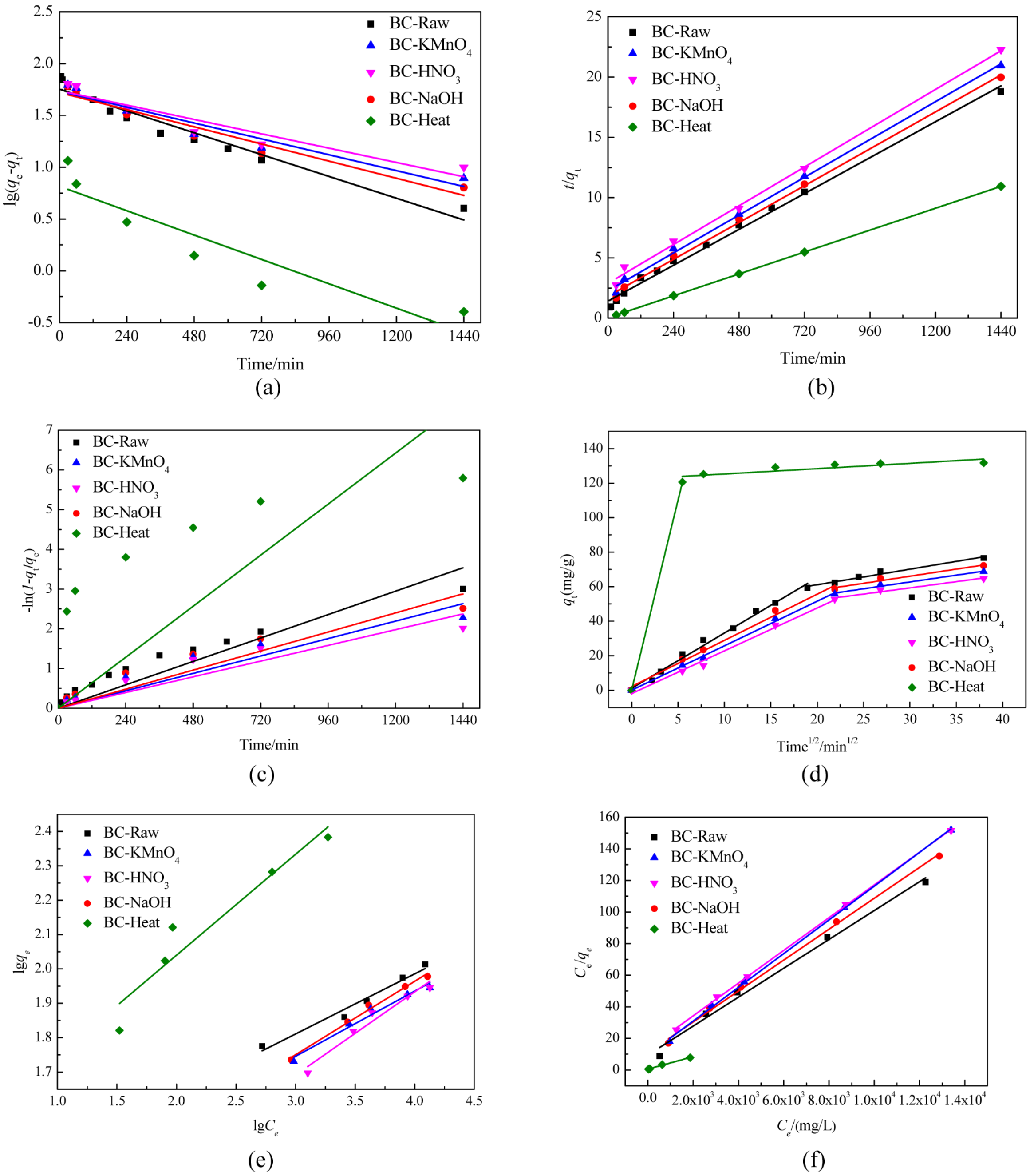

Figure 5. Kinetic and isotherm functions for adsorption of furfural by BCs. (a) Pseudo-first-order model, (b) pseudo-second-order model, (c) film diffusion model, (d) intraparticle diffusion model, (e) Freundlich isotherm, (f) Langmuir isotherm (a, b, c, and d: $T = 298$ K, $m = 75$ g/L, $C_0 = 10$ g/L; e and f: $T = 298$ K, $m = 75$ g/L, $C_0 = 5$ g/L, 8 g/L, 10 g/L, 15 g/L and 20 g/L).

samples are less than 1, suggesting favorable adsorption. Table 5 also shows that all of the rate constants (k) increase from BC-HNO_3 < BC-$KMnO_4$ < BC-NaOH < BC-Raw < BC-Heat, which is in agreement with the order of the furfural uptake.

4. CONCLUSIONS

Renewable bioresources BC and modified BCs were characterized, and adsorptive removal of target component (furfural) by BCs was investigated. Different modification methods resulted in different BC pore structures and surface chemistry. The chemical treatments reduced BC surface area, whereas the heat treatment significantly enlarged the surface area by more than 1 order of magnitude. The hydrophilic and the surface acidic/basic properties of the BC samples were also affected by various treatments. Oxidative treatment of BC produced material with higher hydrophilic and lower electronic density in the carbon matrix. In contrast, the heat treatment almost eliminated the oxygen functional groups, leading to the opposite effect. The adsorption capacities were positively correlated with basicity of the samples in increasing order: BC-HNO_3 < BC-$KMnO_4$ < BC-Raw < BC-Heat, which was also consistent with the hydrophobic trend of the BCs. BC treated by NaOH had the strongest basicity but smallest surface area, exhibiting moderate furfural adsorption capacity, which may be attributed to the conflicting effects of the chemical and physical properties of the sample.

Table 5. Kinetic and Isotherm Parameters for Furfural Removal by BCs

	pseudo-first-order kinetic model		pseudo-second-order kinetic model		
samples	k_1	R^2	k_2	R^2	q_e (mg/g)
BC-Raw	2.02×10^{-3}	0.95	1.09×10^{-4}	0.99	80.58
BC-$KMnO_4$	1.47×10^{-3}	0.92	7.50×10^{-5}	0.99	76.51
BC-HNO_3	1.33×10^{-3}	0.89	6.21×10^{-5}	0.99	74.63
BC-NaOH	1.59×10^{-3}	0.94	8.94×10^{-5}	0.99	78.49
BC-Heat	2.26×10^{-3}	0.81	1.93×10^{-3}	0.99	132.10

	film diffusion model		intraparticle diffusion model					
	k_b	R^2	I_1	$k_{id,1}$	R^2	I_2	$k_{id,2}$	R^2
BC-Raw	2.46×10^{-3}	0.94	1.05	3.21	0.99	42.96	0.90	0.97
BC-$KMnO_4$	1.83×10^{-3}	0.94	−0.12	2.58	0.99	39.02	0.79	0.97
BC-HNO_3	1.65×10^{-3}	0.93	−2.05	2.48	0.99	37.67	0.72	0.95
BC-NaOH	2.00×10^{-3}	0.94	2.04	2.68	0.99	41.33	0.82	0.93
BC- Heat	5.35×10^{-3}	0.71	0.00	22.01	0.99	122.17	0.31	0.98

	Freundlich isotherm			Langmuir isotherm		
	K_F	$1/n$	R^2	K_L	q_m	R^2
BC-Raw	19.35	0.17	0.96	9.77×10^{-4}	109.17	0.99
BC-$KMnO_4$	15.02	0.19	0.97	1.13×10^{-3}	93.55	0.99
BC-HNO_3	9.26	0.24	0.95	7.74×10^{-4}	96.34	0.99
BC-NaOH	12.89	0.21	0.98	9.15×10^{-4}	102.04	0.99
BC- Heat	28.38	0.29	0.89	8.56×10^{-3}	253.16	0.99

In conclusion, chemical treatments, including oxidation treatments with HNO_3 and $KMnO_4$, as well as base treatment with NaOH, inhibit the adsorption of furfural. The heat-treated sample has the highest furfural uptake capacity, with a furfural removal efficiency of nearly 100%, because of its low hydrophilicity, high basicity, and large micropore volume. Therefore, heat treatment is recommended in the application of furfural removal by BC. In addition, the adsorption process of furfural onto the BC and modified BCs can be well described by Ho's pseudo-second-order and intraparticle diffusion kinetic model, suggesting that the rate-limiting step is the adsorbent phase diffusion. The Langmuir isotherm provides a better fitting to the adsorption data compared to the Freundlich isotherm, suggesting the adsorption feature of BCs is mainly a monolayer adsorption. These findings may provide some insight into the modification of BC for fermentation inhibitor removal, and they also demonstrate that optimized biochar adsorbents can be produced by appropriate surface modification for a specific organic compound.

■ AUTHOR INFORMATION

Corresponding Author

*E-mail: wxhwhhy@sina.com.

Notes

The authors declare no competing financial interest.

■ ACKNOWLEDGMENTS

The authors thank the financial supports from the National Natural Science Foundation of China (51376075, 51276075), the National Basic Research Program of China (973 Program: 2013CB228102) and the Special Fund for Agro-scientific Research in the Public Interest (201303095). Mr. Ho Simon Wang has helped improve the manuscript in terms of linguistic presentation.

■ REFERENCES

(1) Sasmal, S.; Goud, V. V.; Mohanty, K. Ultrasound assisted lime pretreatment of lignocellulosic biomass toward bioethanol production. *Energy Fuels* **2012**, *26* (6), 3777−3784.

(2) Kaper, T.; Lager, I.; Looger, L. L.; Chermak, D.; Frommer, W. B. Fluorescence resonance energy transfer sensors for quantitative monitoring of pentose and disaccharide accumulation in bacteria. *Biotechnol. Biofuels* **2008**, *1* (1), 1−10.

(3) Ranjan, R.; Thust, S.; Gounaris, C. E.; Woo, M.; Floudas, C. A.; Keitz, M. V.; Valentas, K. J.; Wei, J.; Tsapatsis, M. Adsorption of fermentation inhibitors from lignocellulosic biomass hydrolyzates for improved ethanol yield and value-added product recovery. *Microporous Mesoporous Mater.* **2009**, *122* (1), 143−148.

(4) Li, L.; Zhang, H. Preparing levoglucosan derived from waste material by pyrolysis. *Energy Source* **2004**, *26* (11), 1053−1059.

(5) Parawira, W.; Tekere, M. Biotechnological strategies to overcome inhibitors in lignocellulose hydrolysates for ethanol production: review. *Crit. Rev. Biotechnol.* **2011**, *31* (1), 20−31.

(6) Sulaymon, A. H.; Ahmed, K. W. Competitive adsorption of furfural and phenolic compounds onto activated carbon in fixed bed column. *Environ. Sci. Technol.* **2007**, *42* (2), 392−397.

(7) Sahu, A. K.; Srivastava, V. C.; Mall, I. D.; Lataye, D. H. Adsorption of furfural from aqueous solution onto activated carbon: Kinetic, equilibrium and thermodynamic study. *Sep. Sci. Technol.* **2008**, *43* (5), 1239−1259.

(8) Singh, S.; Srivastava, V. C.; Mall, I. D. Fixed-bed study for adsorptive removal of furfural by activated carbon. *Colloids Surf., A* **2009**, *332* (1), 50−56.

(9) Lucas, S.; Cocero, M. J.; Zetzl, C.; Brunner, G. Adsorption isotherms for ethylacetate and furfural on activated carbon from supercritical carbon dioxide. *Fluid. Phase Equilib.* **2004**, *219* (2), 171−179.

(10) Gupta, P.; Nanoti, A.; Garg, M.; Goswami, A. The removal of furfural from water by adsorption with polymeric resins. *Sep. Sci. Technol.* **2001**, *36* (13), 2835−2844.

(11) Weil, J. R.; Dien, B.; Bothast, R.; Hendrickson, R.; Mosier, N. S.; Ladisch, M. R. Removal of fermentation inhibitors formed during pretreatment of biomass by polymeric adsorbents. *Ind. Eng. Chem. Res.* **2002**, *41* (24), 6132−6138.

(12) Anbia, M.; Mohammadi, N. A nanoporous adsorbent for removal of furfural from aqueous solutions. *Desalination* **2009**, *249* (1), 150−153.

(13) Sahu, A. K.; Mall, I. D.; Srivastava, V. C. Studies on the adsorption of furfural from aqueous solution onto low-cost bagasse fly ash. *Chem. Eng. Commun.* **2007**, *195* (3), 316−335.

(14) Ahmad, M.; Rajapaksha, A. U.; Lim, J. E.; Zhang, M.; Bolan, N.; Mohan, D.; Vithanage, M.; Lee, S. S.; Ok, Y. S. Biochar as a sorbent for contaminant management in soil and water: A review. *Chemosphere* **2014**, *99*, 19−33.

(15) Mohan, D.; Sarswat, A.; Ok, Y. S.; Pittman, C. U., Jr Organic and inorganic contaminants removal from water with biochar, a renewable, low cost and sustainable adsorbent−a critical review. *Bioresour. Technol.* **2014**, *160*, 191−202.

(16) Li, Y.; Shao, J.; Wang, X.; Yang, H.; Chen, Y.; Deng, Y.; Zhang, S.; Chen, H. Upgrading of bio-oil: Removal of the fermentation inhibitor (furfural) from the model compounds of bio-oil using pyrolytic char. *Energy Fuels* **2013**, *27* (10), 5975−5981.

(17) Yin, C. Y.; Aroua, M. K.; Daud, W. M. A. W. Review of modifications of activated carbon for enhancing contaminant uptakes from aqueous solutions. *Sep. Purif. Technol.* **2007**, *52* (3), 403−415.

(18) Wibowo, N.; Setyadhi, L.; Wibowo, D.; Setiawan, J.; Ismadji, S. Adsorption of benzene and toluene from aqueous solutions onto activated carbon and its acid and heat treated forms: Influence of surface chemistry on adsorption. *J. Hazard. Mater.* **2007**, *146* (1), 237−242.

(19) Wang, L. G.; Yan, G. B. Adsorptive removal of direct yellow 161dye from aqueous solution using bamboo charcoals activated with different chemicals. *Desalination* **2011**, *274* (1), 81−90.

(20) Fan, Y.; Wang, B.; Yuan, S.; Wu, X.; Chen, J.; Wang, L. Adsorptive removal of chloramphenicol from wastewater by NaOH modified bamboo charcoal. *Bioresour. Technol.* **2010**, *101* (19), 7661−7664.

(21) Wang, Y.; Wang, X.; Wang, X.; Liu, M.; Yang, L.; Wu, Z.; Xia, S.; Zhao, J. Adsorption of Pb (II) in aqueous solutions by bamboo charcoal modified with $KMnO_4$ via microwave irradiation. *Colloids Surf., A* **2012**, *414* (20), 1−8.

(22) Wang, X.; Chen, H.; Luo, K.; Shao, J.; Yang, H. The influence of microwave drying on biomass pyrolysis. *Energy Fuels* **2007**, *22* (1), 67−74.

(23) Villacañas, F.; Pereira, M. F. R.; Órfão, J. J. M.; Figueiredo, J. L. Adsorption of simple aromatic compounds on activated carbons. *J. Colloid Interface Sci.* **2006**, *293* (1), 128−136.

(24) Boehm, H. Surface oxides on carbon and their analysis: a critical assessment. *Carbon* **2002**, *40* (2), 145−149.

(25) Liu, Z.; Zhang, F. S. Removal of copper (II) and phenol from aqueous solution using porous carbons derived from hydrothermal chars. *Desalination* **2011**, *267* (1), 101−106.

(26) Zhang, L.; Yu, C.; Zhao, W.; Hua, Z.; Chen, H.; Li, L.; Shi, J. Preparation of multi-amine-grafted mesoporous silicas and their application to heavy metal ions adsorption. *J. Non-Cryst. Solids* **2007**, *353* (44), 4055−4061.

(27) Derylo-Marczewska, A.; Buczek, B.; Swiatkowski, A. Effect of oxygen surface groups on adsorption of benzene derivatives from aqueous solutions onto active carbon samples. *Appl. Surf. Sci.* **2011**, *257* (22), 9466−9472.

(28) Petit, C.; Peterson, G. W.; Mahle, J.; Bandosz, T. J. The effect of oxidation on the surface chemistry of sulfur-containing carbons and their arsine adsorption capacity. *Carbon* **2010**, *48* (6), 1779−1787.

(29) Ania, C.; Parra, J.; Pis, J. Influence of oxygen-containing functional groups on active carbon adsorption of selected organic compounds. *Fuel Process. Technol.* **2002**, *79* (3), 265−271.

(30) López-Garzón, F. J.; Domingo-García, M.; Pérez-Mendoza, M.; Alvarez, P. M.; Gómez-Serrano, V. Textural and chemical surface modifications produced by some oxidation treatments of a glassy carbon. *Langmuir* **2003**, *19* (7), 2838−2844.

(31) Stavropoulos, G.; Samaras, P.; Sakellaropoulos, G. Effect of activated carbons modification on porosity, surface structure and phenol adsorption. *J. Hazard. Mater.* **2008**, *151* (2), 414−421.

(32) Pradhan, B. K.; Sandle, N. Effect of different oxidizing agent treatments on the surface properties of activated carbons. *Carbon* **1999**, *37* (8), 1323−1332.

(33) Ahmad, M.; Lee, S. S.; Rajapaksha, A. U.; Vithanage, M.; Zhang, M.; Cho, J. S.; Lee, S. E.; Ok, Y. S. Trichloroethylene adsorption by pine needle biochars produced at various pyrolysis temperatures. *Bioresour. Technol.* **2013**, *143*, 615−622.

(34) Brown, R. A.; Kercher, A. K.; Nguyen, T. H.; Nagle, D. C.; Ball, W. P. Production and characterization of synthetic wood chars for use as surrogates for natural sorbents. *Org. Geochem.* **2006**, *37* (3), 321−333.

(35) Kuhlbusch, T. Method for determining black carbon in residues of vegetation fires. *Environ. Sci. Technol.* **1995**, *29* (10), 2695−2702.

(36) Chun, Y.; Sheng, G.; Chiou, C. T.; Xing, B. Compositions and sorptive properties of crop residue-derived chars. *Environ. Sci. Technol.* **2004**, *38* (17), 4649−4655.

(37) Yang, H.; Yan, R.; Chen, H.; Lee, D. H.; Zheng, C. Characteristics of hemicellulose, cellulose and lignin pyrolysis. *Fuel* **2007**, *86* (12), 1781−1788.

(38) Yu, C.; Qiu, J. S.; Sun, Y. F.; Li, X. H.; Chen, G.; Zhao, Z. B. Adsorption removal of thiophene and dibenzothiophene from oils with activated carbon as adsorbent: effect of surface chemistry. *J. Porous. Mater.* **2008**, *15* (2), 151−157.

(39) Zhou, J. H.; Sui, Z. J.; Zhu, J.; Li, P.; Chen, D.; Dai, Y. C.; Yuan, W. K. Characterization of surface oxygen complexes on carbon nanofibers by TPD, XPS and FT-IR. *Carbon* **2007**, *45* (4), 785−796.

(40) Boehm, H. Some aspects of the surface chemistry of carbon blacks and other carbons. *Carbon* **1994**, *32* (5), 759−769.

(41) Park, S. J.; Jang, Y. S.; Shim, J. W.; Ryu, S. K. Studies on pore structures and surface functional groups of pitch-based activated carbon fibers. *J. Colloid Interface Sci.* **2003**, *260* (2), 259−264.

(42) Deng, H.; Lu, J.; Li, G.; Zhang, G.; Wang, X. Adsorption of methylene blue on adsorbent materials produced from cotton stalk. *Chem. Eng. J.* **2011**, *172* (1), 326−334.

(43) Moreno-Castilla, C. Adsorption of organic molecules from aqueous solutions on carbon materials. *Carbon* **2004**, *42* (1), 83−94.

(44) Salame, I. I.; Bandosz, T. J. Role of surface chemistry in adsorption of phenol on activated carbons. *J. Colloid Interface Sci.* **2003**, *264* (2), 307−312.

(45) Coelho, C.; Oliveira, A. S.; Pereira, M. F. R.; Nunes, O. C. The influence of activated carbon surface properties on the adsorption of the herbicide molinate and the bio-regeneration of the adsorbent. *J. Hazard. Mater.* **2006**, *138* (2), 343−349.

(46) Geethakarthi, A.; Phanikumar, B. Industrial sludge based adsorbents/industrial by products in the removal of reactive dyes−A review. *Int. J. Water Resour. Environ. Eng.* **2011**, 3 (1), 1−9.

(47) Zhu, M.; Paul, K. W.; Kubicki, J. D.; Sparks, D. L. Quantum chemical study of arsenic (III, V) adsorption on Mn-oxides: Implications for arsenic (III) oxidation. *Environ. Sci. Technol.* **2009**, *43* (17), 6655−6661.

(48) Zhao, W.; Wang, Q. Q.; Liu, F.; Qiu, G. H.; Tan, W. F.; Feng, X. H. Pb^{2+} adsorption on birnessite affected by Zn^{2+} and Mn^{2+} pretreatments. *J. Soils Sedi.* **2010**, *10* (5), 870−878.

(49) Li, L.; Liu, S.; Zhu, T. Application of activated carbon derived from scrap tires for adsorption of Rhodamine B. *J. Environ. Sci.* **2010**, *22* (8), 1273−1280.

(50) Hameed, B.; Rahman, A. Removal of phenol from aqueous solutions by adsorption onto activated carbon prepared from biomass material. *J. Hazard. Mater.* **2008**, *160* (2), 576−581.

(51) Sharma, Y. C.; Upadhyay, S. N. Removal of a cationic dye from wastewaters by adsorption on activated carbon developed from coconut coir. *Energy Fuels* **2009**, *23* (6), 2983−2988.

(52) Nassar, N. N.; Hassan, A.; Pereira-Almao, P. Effect of the particle size on asphaltene adsorption and catalytic oxidation onto alumina particles. *Energy Fuels* **2011**, *25* (9), 3961−3965.